University of Baghdad
College of Engineering
JE
JOURNAL OF ENGINEERING

Journal of Engineering

journal homepage: www.joe.uobaghdad.edu.iq

Volume 29 Number 3 March 2023

Effect of a Parked Car Orientation on a Temperature Distribution and Cooling Load Calculation: Experimental Study

Saman Jalal Salih*
MSc. Student
Dept. of Mechanical Engr.
Salahaddin Univ.
Erbil-Iraq
samanjalal3@gmail.com

Rizgar Bakr Weli
Assist. Prof., PhD
Dept. of Mechanical Engr.
Salahaddin Univ.
Erbil-Iraq
rizgar.weli@su.edu.krd

Hameed D. Lafta
Assist. Prof., Ph.D
Dept. of Mechanical Engr.
Salahaddin Univ.
Sulaimani-Iraq
hameed.lafta@spu.edu.iq

ABSTRACT

When a vehicle is left parked in the sun for an extended period, the gathered heat causes damage to several interiors within the cabin and causes discomfort for people and animals left inside the car. In the present work, the effect of the orientation of a parked white minibus on temperature distribution and cooling load calculation is studied experimentally in an open environment. Two different cases were studied facing south and facing east. For several hours, the temperature inside the car cabin had been monitored and measured at five separate locations. The cooling load calculations are carried out based on the experimental measurements. The results show that the overheating of parked cars always happens as a result of the radiation load especially when a car has a large surface glass area. Also, the ambient load is directly proportional to the ambient temperature, and the total load related directly to radiation load reaches the maximum value of 2358.1 W at 3:00 pm for 1st case and 2118.3 W at 11:00 am for 2nd case which shows an increase of 11.32 %. Thus, these results emphasized the fact that the orientation of the parked car may considerably affect the temperature distribution and the cooling load of the car cabin. Also, the study may be considered an essential step in designing any assisted ventilation or auxiliary air conditioning system that may enhance the car cabin conditions even while the car's engine was off (parked automobile).

Keywords: Solar radiation, car cabin overheating, ambient load, cooling load.

*Corresponding author
Peer review under the responsibility of University of Baghdad.
https://doi.org/10.31026/j.eng.2023.03.07

Article received: 27/11/2022
Article accepted: 18/02/2023
Article published: 01/03/2023

تأثير أتجاه الأشعاع الشمسي على توزيع درجات الحرارة وحساب حمل التبريد داخل سيارة متوقفة : دراسة تجربية

سامان جلال صالح*
طالب ماجستير
جامعة صلاح الدين
اربيل – عراق

رزكار بكر ولى
استاذ مساعد، دكتوراه
جامعة صلاح الدين
اربيل – عراق

حميد دويج لفتة
استاذ مساعد، دكتوراه
جامعة السليمانية التقنية
سليمانية – عراق

الخلاصة

عندما يتم إيقاف سيارة تحت أشعة الشمس المباشرة لفترة طويلة، فإن الحرارة المتراكمة تؤثر على العديد من الأجزاء الداخلية داخل مقصورة السيارة، كما أنها تمثل فترة غير مريحة للركاب والحيوانات التي تركت داخل السيارة وقد يشكل تهديدًا خطيرًا للركاب، ويؤثر على تركيز السائق، ويزيد من احتمالية وقوع حوادث المرور. في الدراسة الحالية تمت دراسة تأثير اتجاه سيارة متوقفة على توزيع درجة الحرارة وحساب حمل التبريد تجريبياً. تم جمع البيانات التجريبية من خلال قياس درجات الحرارة داخل مقصورة السيارة على حافلة بيضاء صغيرة في بيئة مفتوحة. تمت دراسة حالتين مختلفتين، واحدة للجنوب وواحدة للشرق. لعدة ساعات تمت مراقبة درجة الحرارة داخل الحافلة الصغيرة في خمس نقاط منفصلة. تظهر النتائج أن ارتفاع درجة حرارة السيارة المتوقفة يحدث دائمًا نتيجة الحمل الإشعاعي خاصةً عندما تكون السيارة ذات مساحة سطح زجاجي كبير. أيضًا، يتناسب الحمل البيئي طرديًا مع درجة الحرارة المحيطة ويرتبط حمل التبريد الكلي تمامًا بالحمل الإشعاعي الذي يصل إلى الحد الأقصى لقيمة 2358.1 واط عند الساعة 3:00 مساءً للحالة الأولى و2118.3 واط في الساعة 11:00 صباحًا للحالة الثانية. بالإضافة إلى ذلك، أظهر إجمالي حمل التبريد في الحالة الأولى زيادة بنسبة 11.32٪ مقارنة بالحالة الثانية، وقد أكدت هذه النتائج على حقيقة أن اتجاه السيارة المتوقفة قد يكون له تأثير كبير على توزيع درجة الحرارة وحمل التبريد في مقصورة السيارة. ويعتبر العمل الحالي كخطوة اساسية في تصميم اي منظومة تهوية او تبريد بإمكانها ان توفر ظروف مقبولة للمحيط في داخل كابينة المركبة حتى وان كانت المركبة متوقفة عن العمل.

الكلمات الرئيسية: الاشعاع الشمسي، كابينة السيارة الساخنة، الحمل البيئي، حمل التبريد.

1. INTRODUCTION

Traffic accidents are significantly influenced by the interior temperature of cars **(Daanen, et al., 2003)**. When **(Farzaneh and Tootoonchi, 2008)** looked at the impact of ten variables on road accidents in the United States, they found that temperature ranked third. Improved thermal comfort in a car leads to enhanced driver caution, which promotes driving performance and safety in a variety of driving situations. Today's high temperatures are to blame for major environmental problems and global warming. Vehicles are most affected by this temperature when they are parked in direct sunshine for extended periods. Currently, the majority of people choose private transportation over public transit. Parking has been an issue due to the rise of vehicles, particularly in the shopping district. Those who can't park indoors or who want to pay less for parking will have to leave their vehicles in the open area **(Shireesha, et al., 2015)**. The inside temperature of a parked automobile in direct sunshine

can rise by up to 60°C and when parked in direct sunshine, the temperature inside the car's cabin rises to 80 degrees **(Al-Kayiem, et al., 2010)**. Moreover, it produces toxic gases from interior materials' evaporation, thereby increasing health risks for passengers/pets in the cabin **(Setiyo, et al., 2021)**. The driver experiences discomfort for the first 10 minutes due to the overheating inside of the vehicle. The temperature inside a parked automobile may swiftly increase to deadly levels on a warm day, according to research from the Stanford University School of Medicine **(McLaren, et al., 2005)**. The body of the car that is exposed to sunlight is heated in part by solar radiation that passes through the glass and in part by long-wave thermal radiation from the surrounding surfaces. The effective projected area and the solar absorptivity of the body surface will determine how much solar radiation energy will be absorbed by the body **(Simion, et al., 2016)**. Convection (air currents over the body cooling the body by causing evaporation over the skin), conduction (contact heat transfer with other surfaces, such as a car seat), radiation (immediate infrared heat transfer with any visible object or surface at a different temperature than a person's body, such as the sun), or biological processes (such as sweating and exhaling) can all cause heat transfer **(Regnier, 2013)**. As a result of their metal composition and extensive glass surfaces, vehicles experience larger heat gains than buildings. After several hours of parking in a sunny spot, the air and interior surface temperatures of the car quickly increase, which causes several issues. Furthermore, the third biggest contributor to road accidents is extreme temperatures. One of the main causes of collisions is the poor performance of drivers in hot weather **(Hou, et al., 2022)**. Private automobiles have increased in significance as the contemporary economy has progressed. People must leave their vehicles parked in the sun because there aren't enough covered parking spaces. Solar irradiation may cause automobiles to overheat fast, with the cabin air temperature measuring up to (20–30) ^{o}C higher than the outside temperature **(Zhang, et al., 2019)**.

The unsupervised leaving of children in parked automobiles is one of the main causes of fatalities or serious injuries to children in non-traffic incidents with autos. Such a temperature has the potential to pose a serious hazard to occupancy, might impair driver concentration, and increase the likelihood of traffic accidents **(McLaren, et al., 2005)**. Lethal heat strokes cause 37 children to die on average each year in the USA when they are unintentionally left in parked cars **(Lv, et al., 2021)**. The American Automobile Association organization (AAA) in the United States (U.S.) has reported this, and sadly, similar instances also occur in other regions of the world. When a car is stopped and the windows are kept closed, fresh air can't reach the passenger area. Additionally, having kids inside uses up the amount of oxygen. Even on a day with an air temperature of roughly 21°C, this scenario can cause suffocation and the temperature inside the automobile escalates quickly. Due to the underdeveloped thermoregulatory system of a youngster, this condition may result in deadly heatstroke or hyperthermia **(Qawasmi and Taradeh, 2017)**. Particularly in the tropics, this condition gets worse **(Grundstein, et al., 2011)**.

(Mezrhab and Bouzidi, 2006) studied the impacts of solar radiation, glass type, automobile color, and cabin materials on radiative qualities. Both a finite difference approach and a nodal method were used. The compartment was separated into several nodes for solid (i.e., materials) and fluid (i.e., air volume) components. **(Melih Akyol and Kilic, 2010)** presented a dynamic model of an automotive compartment using Matlab-Simulink to investigate the effects of solar irradiation on the interior surfaces of the cabin and the thermal exchanges between the driver and passengers. **(Al-Kayiem, et al., 2010)** carried out experimental and computational research to determine the temperature distribution on the automobile

surfaces and the air cavities in the automobile cabin. They concluded that the dashboard served as a source of convective heat transfer to the nearby air particles as well as a sink for solar radiation. To determine how solar-reflecting automobile shells in either a black or silver hue may lower the soak temperature and A/C capacity, (**Levinson, et al., 2011)** constructed thermal modeling. They found that the silver automobile needs 13% less air conditioning capacity than the black car does to reduce the interior air temperature to 25 °C in 30 minutes. **(Abd-Fadeel, et al., 2013)** investigated the cabin temperature for the hot soak of the automobile passenger compartment under various orientations and discovered that the temperature of the front and back seats remained constant regardless the direction of the car was facing. Based on theoretical heat transfer and integrating thermal inertia **(Marcos, et al., 2014)** created a dynamic thermal model in Matlab for a car cabin. Three scenarios, including some solar radiation, were used to validate the later model. In the same sense, a two-node model for the interior air was included in the transient thermal model of a minibus cabin created by **(Torregrosa-Jaime, et al., 2015)** by using Matlab. In the real tested areas, the Radiant Series Data Method (RTSM) is used to theoretically calculate the cooling demand. **(Joudi and Hussien, 2015)** calculated the cooling load in these measured locations; the theoretically estimated cooling loads are also empirically compared. They found that when a high ventilation rate is applied, it appears from the comparison that the modified Fisher and Pedersen model reduces findings accuracy to 10% or so. (**Aljubury, et al., 2015)** carried out experimental tests to examine the effects of solar radiation on automobile cabin components (dashboard, steering wheel, seat, and inside air) at a location of (33.3 ^{o}N, 44.4 ^{o}E) in Baghdad, Iraq. To ensure the front windscreen received the most (thermal) sun exposure, the test car was directed south. Investigations were done under six distinct parking scenarios. The measurements were taken on summer days with a clear sky beginning at 8 AM and ending at 5 PM. According to the findings, an unprotected parked car's internal air temperature can reach 70 °C and the dashboard temperature can go close to 100 °C. Experimental data under various environmental circumstances, including solar radiation, were used to verify the model. An experimental investigation on thermal comfort in summertime indoor parking, outdoor parking, and outdoor driving settings was carried out by **(Zhou, et al., 2019)**, and the results revealed that the air and surface temperatures within the automobile were temporary and irregular. When the vehicle was parked, the individuals were more sensitive to the temperature environment than when it was moving. (**Hasan, 2020)** looked at how the environment affected the interior space of automobiles in parking spaces. For this goal, two different fabric covers with a 25 mm thermal insulation (Fiber Glass) layer and a 50 mm thick air gap have been devised and produced. The above cover was evaluated on a parked vehicle under the effects of the surrounding in the summer (in Baghdad), and it was discovered that the average temperature of its external surface achieved 61.11 °C, while the average temperature of its internal surfaces attained 75 °C. While using the shield that was easily obtainable locally, the internal surface temperature dropped to 65C°, and by using the suggested shield, the temperature drops to 41 °C. Therefore, the small car's (salon) fuel consumption was decreased by 4.2 liters. (**Chen, et al., 2022)** employed a transient thermal model to investigate the distribution of the heat soak temperature in the passenger compartment under various orientations. In addition, the study examined the impact of four ventilation situations on the infant in the backseat and the driver. The research indicates that the lowest heat load is experienced by the driver and the infant when the car is parked outside, facing east at 14:00, and the surrounding temperature is around 52 ^{o}C. **(Ding, et al., 2022)** examined the impact of open windows on

a vehicle's thermal environment under various environmental circumstances. To conduct a field measurement, two identical vehicles one with and one without window gaps were employed in Beijing's Daxing District. The tests were taken over a 15 days with various window gaps and environmental factors. The findings showed that under high temperatures and intense solar radiation, open windows reduced cabin air temperature by a maximum of 6.7 ^{o}C.

The present experimental study aims to predict and analyze the relationship between car orientation and temperature distribution with ambient thermal loadings and explore their effects on car cabin overheating and cooling load calculations. Also, the study can be considered an essential step in designing any assisted ventilation or auxiliary air conditioning system that may enhance the car cabin conditions even while the car's engine was off (parked automobile).

2. MATHEMATICAL MODELING

An estimate of cooling capacity as a tone of refrigeration may be calculated from the cooling load calculation. Estimating the heating and cooling loads present in a vehicle cabin requires the application of the Heat Balance Method (HBM). For load calculation, mathematical load computation models are developed and assembled from a variety of sources. Under arbitrary parking circumstances, studies input parameters include the simplified shape and typical material characteristics of an automobile. The numerous thermal load categories that may be found in a typical car interior are depicted schematically in **Fig. 1**.

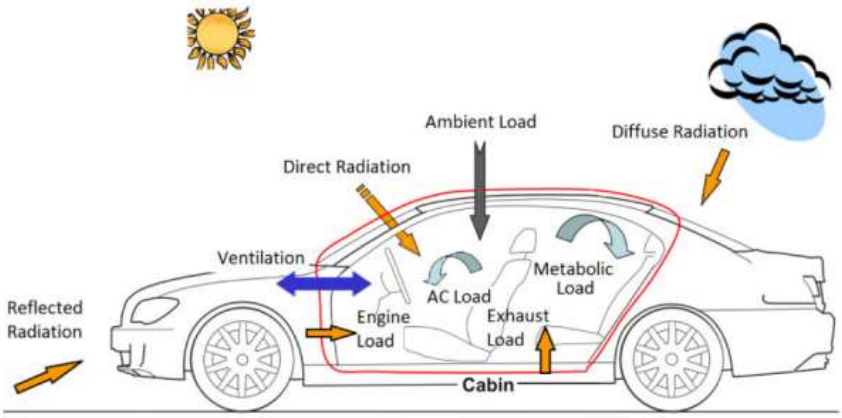

Figure 1. Thermal loads in a typical vehicle cabin **(Fayazbakhsh and Bahrami, 2013).**

A simplified mathematical model of a typical car cabin **(Fayazbakhsh and Bahrami, 2013)**, including nine separate categories, can be used to group the cabin's net heat gain, which may be summed up as:

$$\dot{Q}_{Tot} = \dot{Q}_{Met} + \dot{Q}_{Dir} + \dot{Q}_{Dif} + \dot{Q}_{Ref} + \dot{Q}_{Amb} + \dot{Q}_{Ehx} + \dot{Q}_{Eng} + \dot{Q}_{Ven} + \dot{Q}_{Ac} \quad (1)$$

where:

$\dot{Q}_{Tot}$ is the net overall thermal load encountered by the cabin (W).

$\dot{Q}_{Met}$ is the metabolic load (W).

$\dot{Q}_{Dir}, \dot{Q}_{Dif}, \dot{Q}_{Ref}$ are the direct, diffuse, reflected radiations (W).
$\dot{Q}_{Amb}$ is the ambient load (W).
$\dot{Q}_{Ehx}$, $\dot{Q}_{Eng}$, $\dot{Q}_{Ven}$ are the exhaust, engine, ventilation, and thermal loads (W).
$\dot{Q}_{Ac}$ is the thermal load created by the AC cycle (W).

Depending on a variety of driving factors, the overall load as well as each of these loads may either be positive (heating the cabin) or negative (cooling the cabin). Also, some of the aforementioned loads cross over the body plates or other components of the vehicle, while others are not reliant on the cabin's surface materials. In the case of engine-parked cars, as adopted in the present study, all of the loads can be neglected except the radiation and ambient loads. Accordingly, the calculation of the radiation and ambient loads are given in detail in the subsequent sections.
The following assumption is made of this work **(Zheng, et al., 2011):**
1. The conduction and convection heat load through the body walls and glasses are taken into account.
2. The conduction and convection heat load through celling are neglected.
3. Solar radiation through glasses is considered.
4. The solar radiation through the body wall is neglected.

2.1 Radiation Load

A major section of the cooling loads that cars face is heat gain from solar radiation. Direct, diffuse, and reflected radiation loads can be used to classify the heat load from solar radiation, **(ASHRAE, 2005)**. The amount of incoming solar radiation known as "direct radiation" that immediately hits the surface of a vehicle's body is determined by:

$$\dot{Q}_{Dir} = \sum_{surface} S\tau \dot{I}_{Dir} \cos\theta \quad (2)$$

where
$\dot{I}_{Dir}$ is the direct radiation heat gains per unit area (W/m^2).
θ is the angle between the surface normal and the position of the sun in the sky.
τ: glass transmissivity (0.85).
S is the surface area (m^2).
Simply no radiation loads are taken into consideration before and after local sunrise and sunset, and the direct radiation heat gain per unit area can be calculated by:

$$\dot{I}_{Dir} = \frac{A}{\exp(\frac{B}{\sin\beta})} \quad (3)$$

where β is the altitude angle, which is determined by position and time, and the constants A and B are calculated by the following equations:

$$A = 1160 + (75 * \sin(\frac{360(n-275)}{365}) \quad (4)$$

$$B = 0.174 + (0.035 * \sin(\frac{360(n-100)}{365}) \quad (5)$$

where n is the day number from the 1st of January.

The absorbed diffuse solar radiation consequence for daylight's indirect radiation is calculated by:

$$\dot{Q}_{Dif} = \sum_{surface} S\tau\dot{I}_{Dif} \quad (6)$$

where $\dot{I}_{Dif}$ is the diffuse radiation heat gain per unit area, which is determined by:

$$\dot{I}_{Dif} = C\dot{I}_{Dir}\frac{1+\cos\alpha}{2} \quad (7)$$

α is the surface tilt angle measured from the horizontal surface and C values are constants for various months calculated by:

$$C = 0.095 + (0.04 * \sin(\frac{360(n-100)}{365})) \quad (8)$$

The portion of radiation heat gain that is reflected off the ground and hits the body surfaces of the vehicle is referred to as "reflected radiation." The computed reflected radiation may be calculated by:

$$\dot{Q}_{Dif} = \sum_{surface} S\tau\dot{I}_{Ref} \quad (9)$$

where $\dot{I}_{Ref}$ is the heat gain from the reflected radiation per unit area, it is evaluated as:

$$\dot{I}_{Ref} = (\dot{I}_{Dir} + \dot{I}_{Dif})\rho_g\frac{1-\cos\alpha}{2} \quad (10)$$

where ρ_g is the coefficient of ground reflectivity.

2.2 Ambient Load

The thermal load that is transmitted to the cabin air as a result of the ambient and cabin air temperature differences is known as the ambient load. The overall heat transfers between the environment and the cabin involve outside convection, conduction via body panels, and internal convection. The main structure of the ambient load for the panel and window may be given by:

$$\dot{Q}_{Amb} = \sum_{surface}[S\ U(T_o - T_i)] \quad (11)$$

where
U is the surface element's total heat transfer coefficient (W/m^2.K).
T_i is the typical cabin temperature (^{o}C or K).
T_o is the typical outside temperature (^{o}C or K).
Inside convection, conduction through the surface, and exterior convection are some of the main components that make up U, and it may be formulated as follows:

$$U = \frac{1}{\frac{1}{h_o}+\sum_{layer}\frac{x}{k}+\frac{1}{h_i}} \quad (12)$$

where k is the surface thermal conductivity, h_o and h_i are the outside and inside convection coefficients, and x is the thickness of the wall element.

It is simple to measure the thickness of the vehicle surface and thermal conductivity. **Fig. 2** shows the minibus vehicle layers' details (measured experimentally), given in **Table 1**.

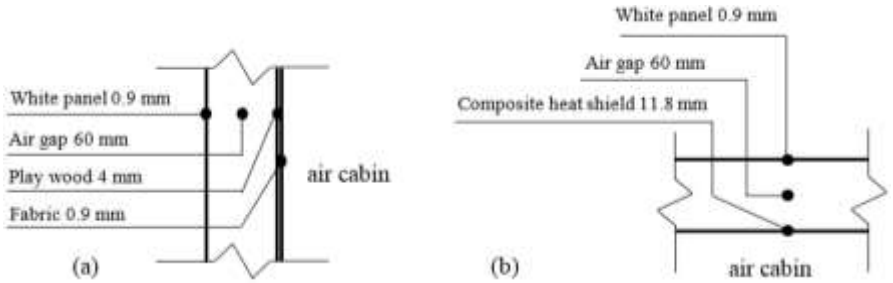

Figure 2. Layers details of (a)-side panels, (b) roof panels

The air velocity and the surface orientation affect the convection heat transfer coefficients h_o and h_i. Consequently, the internal convection heat transfer coefficient (h_i) was assumed to be 25 W/m^2 ^{o}C **(Ružić and Časnji, 2012)** while, for the external convection heat transfer coefficient can be evaluated such that:

$$h_o = 4.65 + 13.96\sqrt{v} \quad (13)$$

where v is the vehicle speed in m/s (for stationary vehicle v=0).

Table 1. Thermal and geometrical properties of the vehicle model.

Material	Thermal conductivity W/m ^{o}C	Layer thickness (mm)	Reference
Tempered single-glass clear	0.8	3 mm	(Ružić and Časnji, 2012)
Metal painted white (roof and side panels)	43	0.9 mm	
Composite heat shield	0.05	11.8 mm	
Fabric	0.65	0.9 mm	(Slavinec, et al., 2016)
Air gap	0.02625	60 mm	(Cengel, et al., 2012)
Play wood	0.1154	4 mm	(Engineered Wood Products Association of Australasia, 2018)

3. EXPERIMENTAL WORK

The heat soak test, as shown in **Fig. 3**, is conducted on a parked white minibus of (1.7 m width x 2.28 m height x 4.6 m length) overall dimensions, such that, in the first case (case 1)

when the minibus was under the sun facing south, and in the second case (case 2) when the minibus was under the sun facing east (case 2).

Figure 3. Minibus under heat soaking test.

The area of the body, including the side panels, and side, rear, and front windows, are given in **Table 2**. The experimental work is carried out from the 19th to 23rd of August 2022, under bright skies, in a shade-free region, and near the Sulaymaniyah meteorological station in Iraq, at 35.6° latitude and 54.4° longitude, the station is situated at an elevation of 882 meters above sea level.

Table 2. Vehicle body details

Vehicle body	Type	Area (m^2)
panel	Roof	5.9
	Side panels	6.688
Glass	Windshield	1.11
	Rear window	0.812
	Left Side window	1.77
	Right side window	1.77

The data acquisition system used to measure the air temperature inside and outside the vehicle is shown in **Fig. 4**. It consists mainly of three parts: the temperature sensor, the data logger, and the software. Six thermocouples of type-k are calibrated to evaluate their performance and accuracy measurement, also, the uncertainty analysis was carried out to determine the percentage error of readings. The statistical analysis shows that the thermocouples temperature measurement has an accuracy of ± 0.01 °C. Such that, the first one was installed outside the automobile cabin to measure the ambient temperature, and the remaining five thermocouples were installed equally spaced into two lines, each line was suspended at (1/3) of the vehicle height in a longitudinal direction of the vehicle, inside the cabin to measure the distribution of the internal temperature. The experiment was performed with the vehicle doors and windows fully closed, and, each test run required more than 11 hours to complete the recording of the data starting at 7:00 AM and ending at 6:00 PM. Dry-bulb outside air temperature is measured, while the global horizontal solar

irradiance was theoretically calculated. The ambient air temperature ranged from 30 °C to 47 °C.

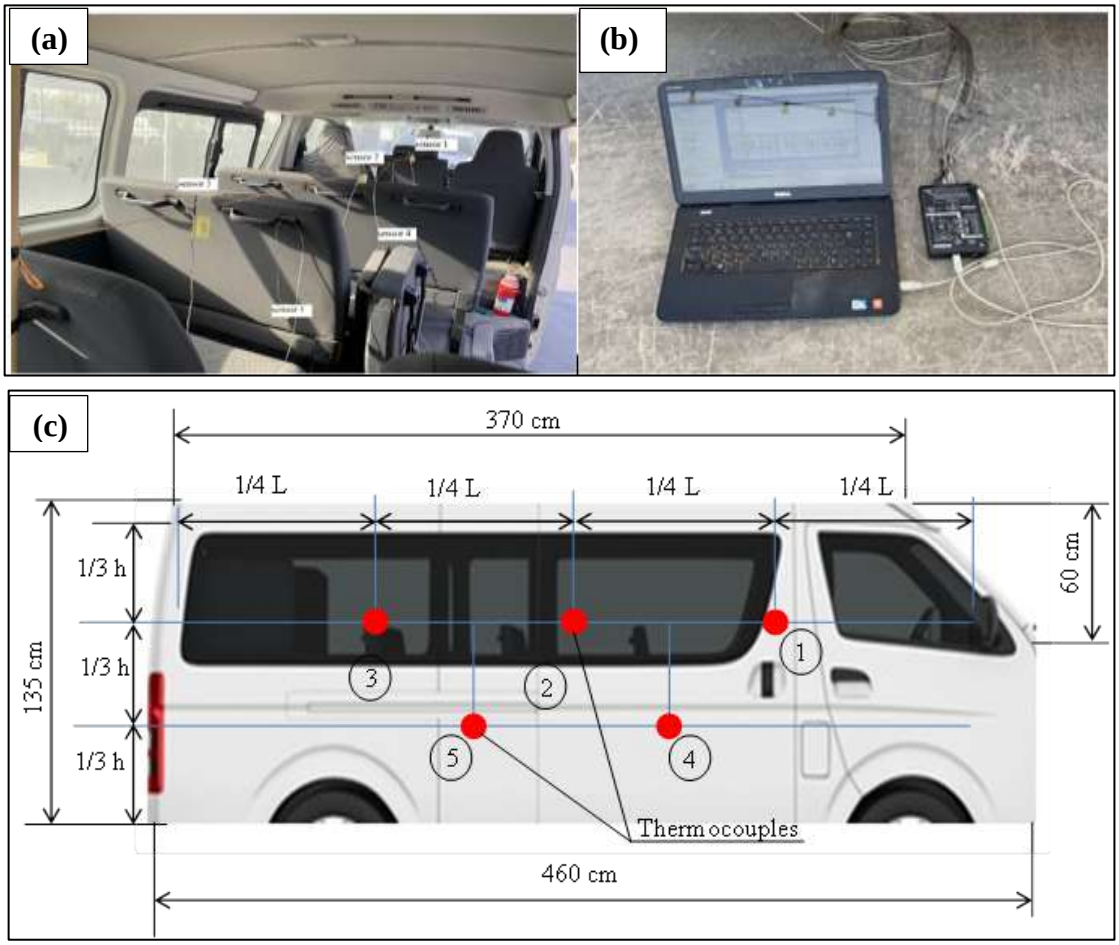

Figure 4. (a) Cabin temperature sensors, (b) data acquisition system.
(c) Bus dimensions and sensor distribution

4. RESULTS AND DISCUSSION

In the current research, the effect of vehicle orientation on temperature distribution and cooling of a parked car was studied experimentally. The cooling load calculation was carried out with adopted assumptions, and the effect of all types of radiation load was considered. MATLAB common software has been used to carry out the simulation.

4.1 Effect of Radiation and Ambient Loads on Vehicle Cabin Temperature

Iraq is amongst those countries where the sun warms the surface of the earth the whole year. **Fig. 5** shows the sun's path and the altitude angle of the sun during the year of the Sulaymaniyah meteorological station in Iraq, at 35.6° latitude and 54.4° longitude. Also, the figure demonstrates that the daylight length is about 9 to 16 hours during the year and it has the maximum daylight in June.

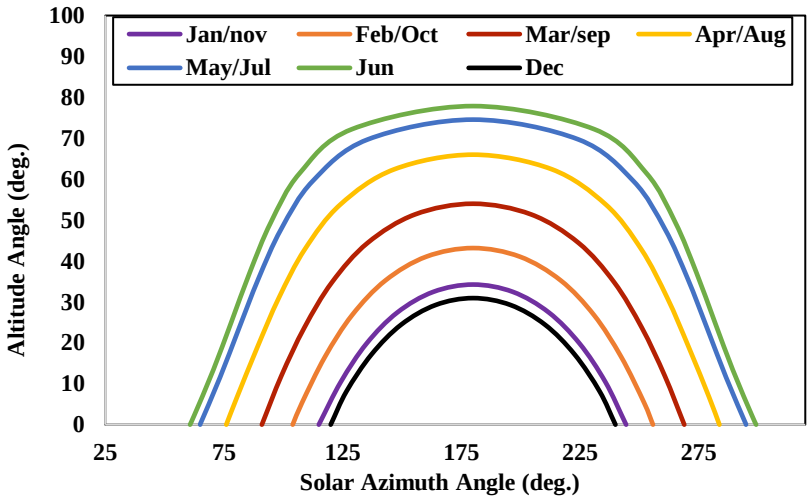

Figure 5. Sun path chart.

The variation of the direct, defused, and reflected radiations on the horizontal surface for the current study on the 22nd of August, 2022, are shown in **Fig. 6**. A transient temperature variation experiment has conducted on a day from 7:00 am to 6:00 pm under the hot sun in the open car parking to measure the temperatures inside the car. Initially, the temperature has measured inside and outside of the car experimentally.

Figs. 7 and **8** show the car cabin's outside and inside temperature history. It can be observed that the ambient temperature for the first case climbed from 32 to 47 °C (31.91% increase) at 2:30 pm then it reduces to 42 °C (10.64% decrease). For the second case, the ambient temperature moderately rises from 30 to 45 °C (33.33% increase) at 3:00 pm then it is minimally dropped to 39 °C (13.33% decrease).

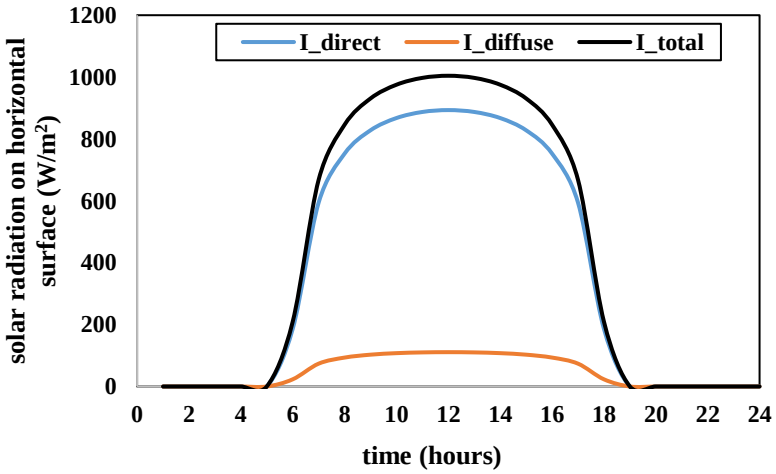

Figure 6. Variation of direct, diffused, and total load on a horizontal surface with time.

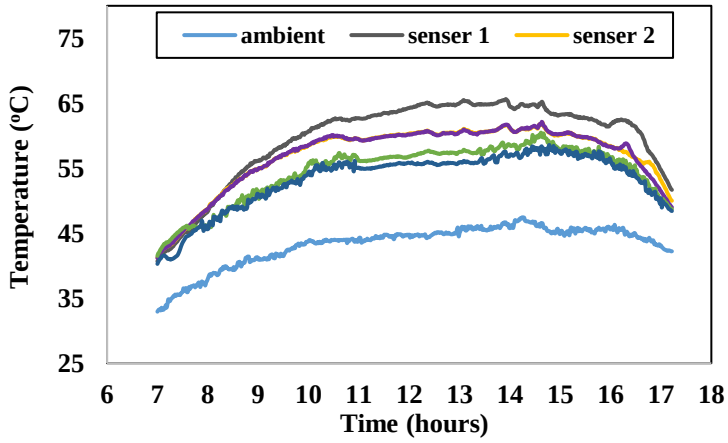

Figure 7. Variation of ambient and cabin temperatures with time measured during the test for 1st case (facing south).

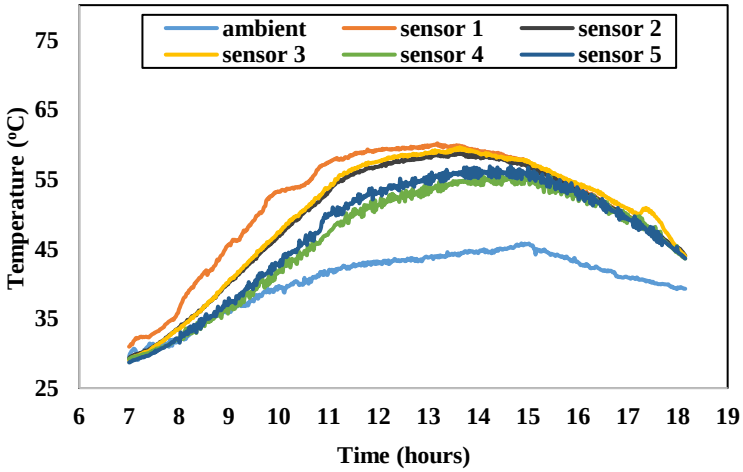

Figure 8. Variation of ambient and cabin temperatures with time measured during the test for 2nd case (facing east).

It is noted that with increasing the ambient temperature, the cabin car temperature also increases. Compared to the sensor near the dashboard (sensor 1), those situated behind the driver's seat (sensors 2 and 3) are less vulnerable to sun radiation, and the peak temperature reported for sensor 1 for 1st and 2nd cases is (65.65 and 60.15) °C, respectively. In the same sense, the sensors located in the upper zone detect high-temperature values compared with the sensors positioned beneath them. The readings of the sensors, in particular, clearly reveal that there is a considerable temperature difference inside the car interior compared with the outside one. The drivers and passengers will also feel this temperature difference. As well as, after solar radiation and ambient temperature begin to fall, the thermal mass of the vehicle keeps the cabin air temperature at an elevated level.

4.2 Effect of Vehicle Orientation on a Cabin Cooling Load

Figs. 9 and **10** explore the effect of the ambient temperature variation and vehicle orientation (facing) on the vehicle cabin temperature daily variation;

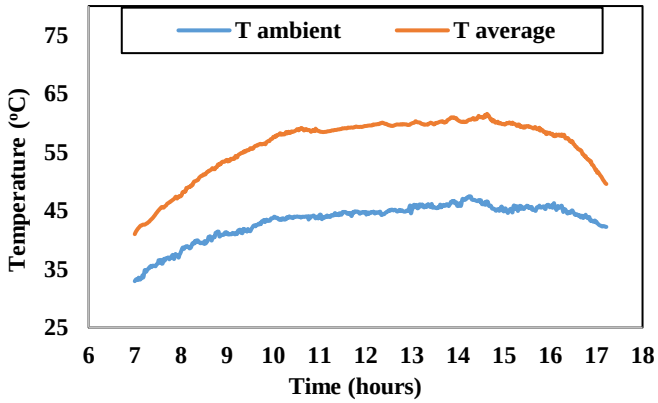

Figure 9. Variation of the average temperature of the car cabin with time for 1st case (facing south).

The results show that the average inside temperature (average of five thermocouples reading) of the car cabin depends mainly upon the ambient temperature, and the maximum recorded temperature differences for the first case and the second case are 15.7 and 13.8 °C respectively.

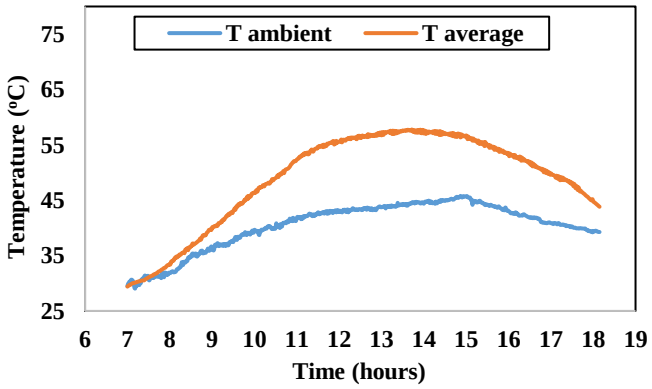

Figure 10. Variation of the average temperature of the car cabin with time for 2nd case (facing east).

Figs. 11 and **12** show the effect of vehicle orientation on the variation of the radiation loads (direct, diffused, and reflected) and the total radiation load with time.

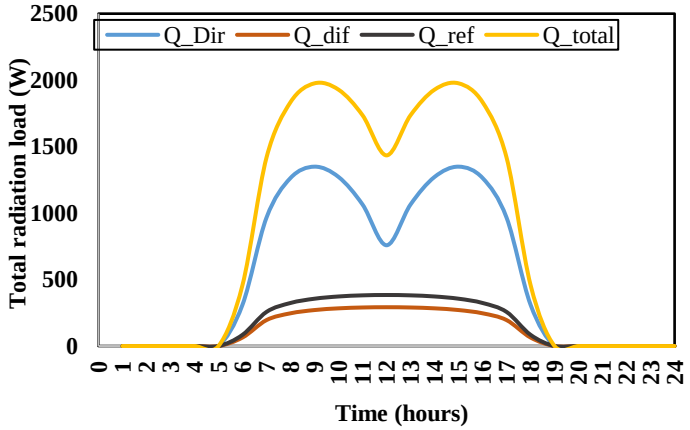

Figure 11. Variation of the radiation load with the time for 1st case (facing south).

At 12:00 pm the diffused and reflected load have their maximum values. While, unlike the direct radiation load, the diffused and reflected load don't have definite directions to the surface, thus, the direct radiation load has the maximum values of 1349.14 W at 9:00 am and 3:00 pm. It is attributed to the fact that in 1st case when the car faces south, the side area of the car glass will receive the maximum direct radiation load two times at 9:00 am and 3:00 pm. While, in 2nd case, the direct radiation load reached its maximum value of 1165.4 W at 10:00 am, because when the car faces east the tilted windshield glass angle of 50° with horizontal will receive the maximum direct radiation load than other glass windows. Finally, the direct radiation load has the most significant effect on the total radiation load is noted. So the total radiation load gets the maximum value of 1976.01 W and 1830.5 W at 3:00 pm and 11:00 am for both cases respectively.

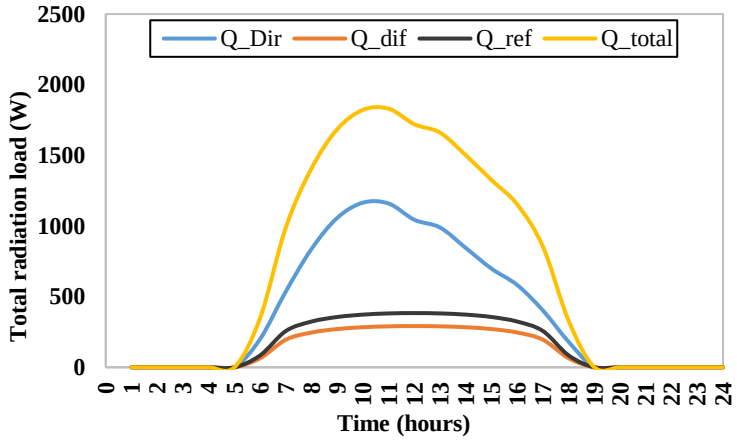

Figure 12. Variation of the radiation load with the time for 2nd case (facing east).

The total ambient load is directly proportional to ambient temperature, i.e higher ambient temperature results in a greater ambient load as depicted in **Fig. 13**. Therefore, the ambient load has a maximum value of 382.1 W at the maximum ambient temperature of 45 °C at 3:00 pm. after that the ambient temperature gradually fell, hence, the ambient load also declined.

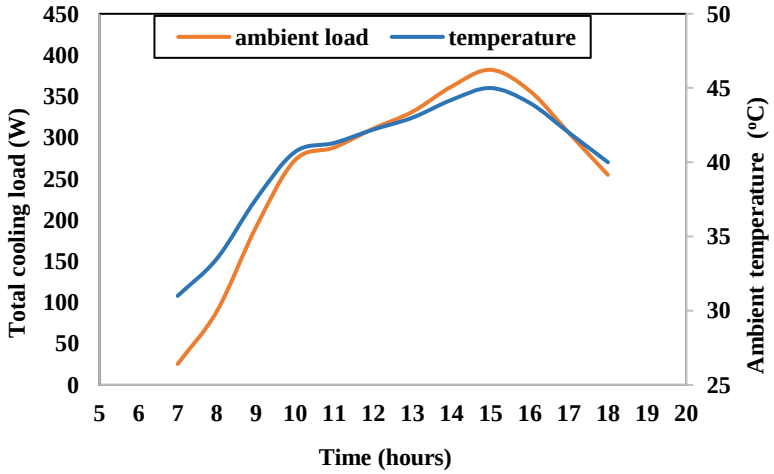

Figure 13. Variation of the ambient load and temperature with time.

The overall cooling load for a parked car is completely related to the radiation load which reaches the maximum value of 2358.1 W at 3:00 pm for 1st case and 2118.3 W at 11:00 am for 2nd case as shown in **Fig. 14**. Thus, the total cooling load in the first case shows an increase of 11.32 % compared with that of the second case and nevertheless the radiation load has the maximum values for both cases at the same time during daylight.

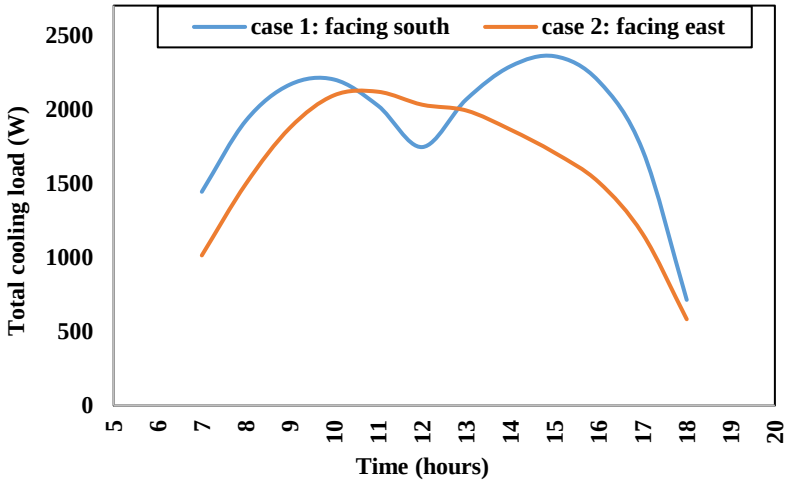

Figure 14. Variation of the total cooling load with the time.

The ambient temperatures, ambient loads, radiation loads, and total cooling loads are depicted in **Table 3** for different vehicle orientations (south facing and east facing).

Table 3. Total cooling load calculation

Time (hour)	Temperature (°C)	Ambient load (W)	Radiation load (W)		Total cooling load (W)	
			Case 1 (facing south)	Case 2 (facing east)	Case 1 (facing south)	Case 2 (facing east)
7:00	31	25.47	1417.89	988.36	1443.36	1013.835
8:00	33.5	89.16	1834.34	1407.85	1923.5	1497.011
9:00	37.5	191.05	1976.01	1684.45	2167.06	1875.509
10:00	40.7	272.57	1928.31	1822	2200.88	2094.578
11:00	41.3	287.86	1735.84	1830.5	2023.70	2118.362
12:00	42.2	310.78	1434.1	1719.99	1744.88	2030.779
13:00	43	331.16	1735.84	1660.6	2067	1991.769
14:00	44.2	361.73	1928.31	1501.03	2290.04	1862.769
15:00	45	382.11	1976.01	1325.01	2358.12	1707.128
16:00	44	356.64	1834.34	1152.43	2190.98	1509.074
17:00	42	305.69	1417.89	853.63	1723.58	1159.325
18:00	40	254.74	458.98	328.29	713.72	583.0354

5. CONCLUSIONS

The variation of the temperature of the cabin of a minibus has been evaluated experimentally for different orientations of a parked automobile and the thermal loads due to ambient and radiation loads are calculated based on the experimental data of the measured temperatures.

1- Overheating a parked vehicle always happens as a result of the radiation load especially when a car has a large surface glass area, and this produces more radiation load, thus a greater cooling load is required.

2- The ambient load is directly proportional to the ambient temperature and the total cooling load is completely related to the radiation load.

3- The total cooling load reaches the maximum value of 2358.1 W at 3:00 pm for the 1st case and 2118.3 W at 11:00 am for the 2nd case.

4- Based on the temperature variation of the vehicle cabin, the best face for parked cars before midday is when the vehicle front faces the west- direction, while, in the afternoon the vehicle front faces the east direction.

5- As well as, the total cooling load in the first case (facing south) shows an increase of 11.32 % compared with that of the second case (facing east).

6- The experimental results emphasized the fact that the orientation of the parked car may considerably affect the temperature distribution and the cooling load of the parked car cabin.

NOMENCLATURE

Symbol	Description	Symbol	Description
A	Constant, W/m^2.	$\dot{Q}_{Ehx}$	Exhaust loads, W.
B	Constant	$\dot{Q}_{Eng}$	Engine loads, W.
C	Constant.	$\dot{Q}_{Ven}$	Ventilation and thermal loads, W.
h_o	Outside convection coefficients, W/m^2 ^{o}C.	$\dot{Q}_{Ac}$	Thermal load created by the AC cycle, W
h_i	Inside convection coefficients, W/m^2 ^{o}C.	S	Surface area, m^2.
$\dot{I}_{Dif}$	Diffuse radiation, W/m^2	Ti	Cabin temperature, ^{o}C.
$\dot{I}_{Dir}$	Direct radiation heat gains per unit area, W/m^2.	To	Outside temperature, ^{o}C.
$\dot{I}_{Ref}$	Reflected radiation, W/m^2.	v	Vehicle speed, m/s.
k	Thermal conductivity, W/m ^{o}C.	U	Heat transfer coefficient, W/m^2 ^{o}C
n	Number of the day.	x	The thickness of the surface element, mm.
$\dot{Q}_{Tot}$	Net overall thermal load, W	α	Surface tilt angle, deg
$\dot{Q}_{Met}$	Metabolic load, W.	β	Altitude angle, deg.
$\dot{Q}_{Dir}$	Direct radiations, W.	ρ_g	Ground reflectivity.
$\dot{Q}_{Dif}$	Diffuse radiations, W.	τ	Surface element transmissivity
$\dot{Q}_{Ref}$	Reflected radiations, W.	θ	The angle between the normal surface and the position of the sun in the sky, deg.
$\dot{Q}_{Amb}$	Ambient load, W.		

REFERENCES

Abd-Fadeel, W.A., and Hassanein, S.A., 2013. Temperature variations in a parked car exposed to direct sun during hot and dry climates. *International Journal of Automobile Engineering Research & Development*, 3(1), pp. 75-80.

Al-Kayiem, H.H., Sidik, M.F.B.M., and Munusammy, Y.R., 2010. Study on the thermal accumulation and distribution inside a parked car cabin. *American Journal of Applied Sciences*, *7*(6), pp. 784-789.

Aljubury, I.M.A., Farhan, A.A., and Mussa, M.A., 2015. Experimental study of interior temperature distribution inside parked automobile cabin. *Journal of Engineering*, *21*(3), pp. 1-10.

ASHRAE, 2005. Fundamentals, Inch-Pound Edition. Atlanta, GA: American Society of Heating, Refrigerating and Air-Conditioning. Handbook.

Cengel, Y., Cimbala, J., and Turner, R., 2012. *EBOOK: Fundamentals of Thermal-Fluid Sciences (SI units)*. McGraw Hill.

Chen, S., Du, B., Li, Q., and Xue, D., 2022. The influence of different orientations and ventilation cases on temperature distribution of the car cabin in the hot soak. *Case Studies in Thermal Engineering*, *39*, p. 102401. doi:10.1016/j.csite.2022.102401.

Daanen, H.A., Van De Vliert, E., and Huang, X., 2003. Driving performance in cold, warm, and thermoneutral environments. *Applied ergonomics*, *34*(6), pp. 597-602. doi:10.1016/S0003-6870(03)00055-3.

Ding, X., Zhang, W., Yang, Z., Wang, J., Liu, L., Gao, D., Guo, D., and Xiong, J., 2022. Effect of Open-Window Gaps on the Thermal Environment inside Vehicles Exposed to Solar Radiation. *Energies*, *15*(17), p.6411. doi:10.3390/en15176411.

Engineered Wood Products Association of Australasia. 2018. Facts About Plywood [online]: EWPAA. Available at: https://dokumen.tips/documents/ewpaa-f-a-p-lvl-pngfp-facts-about-plywood-lvl-understanding-the-characteristics.html?page=1 [Accessed 1/11/2022.

Farzaneh, Y., and Tootoonchi, A.A., 2008. Controlling automobile thermal comfort using optimized fuzzy controller. *Applied Thermal Engineering*, *28*(14-15), pp. 1906-1917. doi:10.1016/j.applthermaleng.2007.12.025.

Grundstein, A., Null, J., and Meentemeyer, V., 2011. Weather, geography, and vehicle-related hyperthermia in children. *Geographical Review*, *101*(3), pp. 353-370. doi: 10.1111/j.1931-0846.2011.00101.

Hasan, A.A., 2020. Suggestion of New Double Layers Car Covers to Reduce the Environment Effect on Car Cabin through Parked Unshaded Area. *Al-Rafidain University College for Sciences*, (47).

Hou, K., Zhang, L., Xu, X., Yang, F., Chen, B., and Hu, W., 2022. Ambient temperatures associated with increased risk of motor vehicle crashes in New York and Chicago. *Science of the total environment*, *830*, p. 154731. doi:10.1016/j.scitotenv.2022.154731.

Joudi, K.A., and Hussien, A.N., 2015. Internal Convective Heat Transfer Effect on Iraqi Building Construction Cooling Load. *Journal of Engineering*, *21*(9), pp. 119-134.

Levinson, R., Pan, H., Ban-Weiss, G., Rosado, P., Paolini, R., and Akbari, H., 2011. Potential benefits of solar reflective car shells: Cooler cabins, fuel savings and emission reductions. *Applied Energy*, *88*(12), pp. 4343-4357. doi:10.1016/j.apenergy.2011.05.006.

Lv, Y., Huang, A., Yang, J., Xu, J., and Yang, R., 2021. Improving cabin thermal environment of parked vehicles under direct sunlight using a daytime radiative cooling cover. *Applied Thermal Engineering*, *190*, p. 116776. doi:10.1016/j.applthermaleng.2021.116776.

Marcos, D., Pino, F.J., Bordons, C., and Guerra, J.J., 2014. The development and validation of a thermal model for the cabin of a vehicle. *Applied Thermal Engineering*, *66*(1-2), pp. 646-656. doi:10.1016/j.applthermaleng.2014.02.054.

McLaren, C., Null, J., and Quinn, J., 2005. Heat stress from enclosed vehicles: moderate ambient temperatures cause significant temperature rise in enclosed vehicles. *Pediatrics*, *116*(1), pp. e109-e112. doi:10.1542/peds.2004-2368.

Melih Akyol, S., and Kilic, M., 2010. Dynamic simulation of HVAC system thermal loads in an automobile compartment. *International journal of vehicle design*, *52*(1-4), pp. 177-198. doi:10.1504/IJVD.2010.029643.

Mezrhab, A., and Bouzidi, M., 2006. Computation of thermal comfort inside a passenger car compartment. *Applied thermal engineering*, *26*(14-15), pp. 1697-1704. doi:10.1016/j.applthermaleng.2005.11.008.

Qawasmi, A., and Taradeh, N., 2017. Smart automobile air conditioning and ventilation system.

Regnier, C., 2013. Guide to setting thermal comfort criteria and minimizing energy use in delivering thermal comfort.

Ružić, D., and Časnji, F., 2012. Thermal interaction between a human body and a vehicle cabin. *Heat Transfer Phenomena and Applications, Rijeka: InTech*, pp. 295-318. doi:10.5772/51860.

Setiyo, M., Waluyo, B., Widodo, N., Rochman, M.L., Munahar, S., and Fatmaryanti, S.D., 2021. Cooling effect and heat index (HI) assessment on car cabin cooler powered by solar panel in parked car. *Case Studies in Thermal Engineering*, *28*, p. 101386. doi:10.1016/j.csite.2021.101386.

Shireesha, Y., Karthik, S., and Ch Mohan, L.V.N., 2015. Comparison of Different Car Cooling Systems with Portable Car Cooling System. *IOSR Journal of Mechanical and Civil Engineering Ver. V. doi:10.9790/1684-12255057*.

Simion, M., Socaciu, L., and Unguresan, P., 2016. Factors which influence the thermal comfort inside of vehicles. *Energy Procedia*, *85*, pp. 472-480. doi:10.1016/j.egypro.2015.12.229.

Slavinec, M., Repnik, R., and Klemenčič, E., 2016. The impact of moisture on thermal conductivity of fabrics. *Anali Pazu*, *6*(1-2), pp. 8-12. doi:10.18690/analipazu.6.1-2.8-12.2016.

Torregrosa-Jaime, B., Bjurling, F., Corberán, J.M., Di Sciullo, F., and Payá, J., 2015. Transient thermal model of a vehicle's cabin validated under variable ambient conditions. *Applied Thermal Engineering*, *75*, pp. 45-53. doi:10.1016/j.applthermaleng.2014.05.074.

Zhang, S., He, W., Chen, D., Chu, J., Fan, H., and Duan, X., 2019. Thermal comfort analysis based on PMV/PPD in cabins of manned submersibles. *Building and Environment*, *148*, pp. 668-676. doi:10.1016/j.buildenv.2018.10.033.

Zheng, Y., Mark, B., and Youmans, H., 2011. *A simple method to calculate vehicle heat load* (No. 2011-01-0127). SAE Technical Paper. doi:0.4271/2011-01-0127.

Zhou, X., Lai, D., and Chen, Q., 2019. Experimental investigation of thermal comfort in a passenger car under driving conditions. *Building and Environment, 149*, pp. 109-119. doi:10.1016/j.buildenv.2018.12.022.